AMP-activated protein kinase activator A-769662 increases intracellular calcium and ATP release from astrocytes in an AMPK-independent manner

Julia M. Vlachaki Walker[1,2], Josephine L. Robb[1], Ana M. Cruz[1], Amrinder Malhi[1], Paul G. Weightman Potter[1], Michael L.J. Ashford[2], Rory J. McCrimmon[2], Kate L.J. Ellacott[1], Craig Beall[1,2]

[1]Institute of Biomedical and Clinical Sciences, University of Exeter Medical School, RILD Building, Barrack Road, Exeter, EX2 5DW, UK

[2]Division of Molecular and Clinical Medicine, Ninewells Hospital and Medical School, University of Dundee, Dundee, DD1 9SY, UK

Corresponding Author:

Craig Beall

Institute of Biomedical and Clinical Sciences, University of Exeter Medical School, RILD Building, Barrack Road, Exeter, EX2 5DW, UK

01392 408209

Email: c.beall@exeter.ac.uk

Keywords: AMPK, ATP, A-769662, intracellular calcium, U373, hypothalamic astrocytes, cortical astrocytes, GT1-7, SH-SY5Y, BV-2, H4IIE, C2C12, INS-1

Abstract word count: 250

Main body word count: 3441

Number of references: 35

Tables: 0

Figures: 5 (+ 5 supplementary figures)

Supplementary methods

Abstract

Aim: Astrocytes are the main sources of extracellular ATP (eATP) within the brain, which functions as a gliotransmitter, capable of modulating neuronal and astrocytic activity. These cells play an important role in regulating energy homeostasis partly via astrocyte-derived ATP. Given the role of AMPK in regulating intracellular ATP levels, we hypothesised that AMPK may alter ATP release from astrocytes.

Methods: Measurements of ATP release were made from human U373 astrocytoma cells, primary mouse hypothalamic (HTAS) and cortical astrocytes (CRTAS) and wild type and AMPK α1/α2 null mouse embryonic fibroblasts (MEFs). Cells were treated with drugs known to modulate AMPK activity: A-769662, AICAR and metformin, for up to 3 hours. Intracellular calcium was measured using Fluo4 and Fura-2 calcium-sensitive fluorescent dyes.

Results: In U373 cells, A-769662 (100 μM) increased AMPK phosphorylation, whereas AICAR and metformin (1 mM) induced a modest increase or had no effect, respectively. Only A-769662 increased extracellular ATP (eATP) levels, which was partially blocked by AMPK inhibitor Compound C. A-769662-induced increases in eATP were preserved in AMPK α1/α2 null MEF cells. A-769662 increased intracellular calcium in U373, HTAS and CRTAS cells and chelation of intracellular calcium using BAPTA-AM reduced A-769662-induced eATP levels. A-769662 also increased ATP release from a number of other central and peripheral endocrine cell types.

Conclusions: AMPK is required to maintain basal eATP levels but is not required for A-769662-induced increases in eATP. A-769662 (>50 μM) enhanced

intracellular calcium levels leading to ATP release in an AMPK and purinergic receptor independent pathway.

Introduction:

AMP-activated protein kinase (AMPK) is a cellular and whole body energy sensor involved in the regulation of energy homeostasis (for recent review see[1]). Structurally, AMPK is a heterotrimer composed of α, β and ϒ-subunits. The α-subunit, which has two isoforms AMPKα1 and α2, contains the catalytic domain required for kinase activity. The regulatory β- and ϒ-subunits subunits have two and three isoforms, respectively, with one isoform of each required as a scaffold for binding the catalytic domain of the kinase. Once active, AMPK switches off energy consuming pathways such as fatty acid synthesis, by phosphorylating and inhibiting acetyl CoA carboxylase (ACC)[2], and protein translation via inhibition of the mammalian target of rapamycin (mTOR) pathway[3]. AMPK also stimulates energy production, for example by increasing glucose uptake[4], with the net effect of maintaining intracellular ATP levels.

Within the brain, AMPK is an important regulator of whole body glucose and energy homeostasis. Enhancement of AMPK activity in the arcuate nucleus increases food intake in mice and AMPK forms part of the signaling pathway by which leptin inhibits food intake[5]. Conversely, orexigenic hormones such as ghrelin require AMPK to stimulate food intake[6]. AMPK also plays a central role in glucose homeostasis as pharmacological activation of the kinase using AICAR can augment the counterregulatory response to insulin-induced hypoglycaemia in rats[7].

To date most research on the role of AMPK in the central nervous system (CNS) has focused on neurons; however, glial cells such as oligodendrocytes, microglia

and astrocytes also contain AMPK, yet little is currently known about its function within these cells. Astrocytes play important supporting roles for neurons partly through releasing gliotransmitters into the extracellular space, such as ATP (for review see [8]). In the brain, enhanced extracellular ATP (eATP) levels are widely accepted as a ubiquitous stress signal[8], for example capable of initiating inflammatory signalling cascades by activating purinergic receptors (P2R)[9]. Several pieces of data suggest a potential role for glial-derived eATP in the regulation of whole body energy/glucose homeostasis that could be modulated by glial AMPK. Firstly, obesity is associated with glial cell activation in mice[10-12] and humans[13] and recent data suggests that glia play a role in regulating feeding behaviour[14-17]. Astrocyte-derived eATP is broken down within the extracellular space to adenosine, which, via activation of the adenosine A1 receptor, inhibits the activity of hypothalamic agouti-related (AgRP) protein neurons, which are critical for the regulation of food intake[18]. This provides evidence for ATP, acting as a gliotransmitter, to modulate energy homeostasis. Moreover, microglia can be activated by eATP leading to initiation of the NF-κB signalling cascade and production of pro-inflammatory cytokines[9], with NF-κB signalling in neurons and glia playing an important role in the regulation of energy homeostasis[19, 20]. Pro-inflammatory cytokine signalling is directly involved in the central control of energy homeostasis as intracerebroventricular injection of TNFα acutely inhibits food intake in rats[21]. Extracellular ATP is also neuromodulatory via activation of Ca^{2+}-permeable P2X receptors and has been shown to excite hypothalamic steroidogenic factor 1 (SF-1) neurons, which are involved in the regulation of food intake[22].

Given the importance of eATP in regulating myriad processes within the brain and the role of AMPK in regulating intracellular ATP levels, we hypothesized that AMPK may regulate eATP levels by blocking or reducing ATP release from astrocytes, thus maintaining intracellular ATP for metabolism. We tested this hypothesis *in vitro* by examining ATP release from human U373 astrocytoma cells and mouse primary hypothalamic and cortical astrocytes using the structurally distinct activators of AMPK, A-769662, AICAR and metformin. We conclude that only A-769662 alters eATP levels, which is mediated by increased release of calcium from intracellular stores, in a cell autonomous manner.

Materials and Methods

Chemicals

A-769662, AICAR and metformin were purchased from Tocris (Bristol, UK). A-769662 was dissolved in DMSO (applied at a maximum volume:volume ratio of 0.1%). AICAR and metformin were dissolved in water.

Cell culture

U373 cells were purchased from Public Health England. Primary mouse astrocytes were isolated from neonatal mice P1-5 and validated as astrocyte-enriched cultures of >80% GFAP-positive cells. Cultures contained less than 2% Iba1-positive microglial cells (ESM Figure 1). Wild type (WT) and AMPKα1/α2 null MEF cells were a kind gift from Dr Benoit Viollet. All cell cultures were grown in stock media (DMEM, Sigma, UK) supplemented with 10% Hyclone FBS (ThermoFisher, UK) containing 25 mM glucose. Cells were seeded the day prior to experimentation and grown in media containing 7.5 mM glucose (sufficient to prevent glucose depletion overnight), supplemented with 10% FBS, with the exception of MEF cells, which were maintained in 25 mM glucose containing media. On the day of experimentation, cells were cultured in serum-free media (Gibco, UK) containing 2.5 mM glucose, a physiologically-relevant brain glucose concentration, for 2 hours before treatment (up to 3 hours).

Immunoblotting

Cells were grown to 60-70% confluence in 60 mm dishes. Protein was isolated using lysis buffer, protein concentrations determined by the method of Bradford and lysates subjected to SDS-PAGE and electrotransferred to nitrocellulose

membrane. Proteins (total and phosphorylated) were immunoblotted and identified using infrared fluorescence using the Licor Odyssey scanner (see supplementary methods for antibody details).

Determination of ATP concentrations

Extracellular and intracellular ATP levels were determined using ATPLite two-step (PerkinElmer, UK) as per the manufacturer's instructions, with minor modifications (see supplementary methods).

Calcium imaging

Intracellular calcium was measured using either Fluo4 Direct (ThermoFisher, UK) using a Pherastar FS plate reader or Fura-2 (Life Technologies, UK) for single cell calcium imaging (see supplementary methods).

Assessment of cellular metabolism

Oxygen consumption rate (OCR) and extracellular acidification rate (ECAR) of U373 cells was assessed using a Seahorse Bioscience XFe96 extracellular flux analyser (see supplementary methods for assay conditions).

Statistical analysis

A one-sample t-test was used to determine significant changes in phosphorylation, relative to control. For comparisons of two groups an unpaired t-test was used and for multiple group comparisons, a one-way ANOVA with post-hoc Bonferroni were used. Statistical tests performed using GraphPad Prism software (Prism 5; GraphPad Software, La Jolla, CA, USA). Results are expressed as mean ± standard

error, unless otherwise stated. p values of <0.05 were considered statistically significant.

Results

A-769662 potently activates AMPK and stimulates ATP release from human U373 astrocytoma cells

U373 astrocytoma cells were treated for 30 minutes (Fig. 1A-D) or 3 hours (Fig. 1E-H) with compounds reported to activate AMPK: A-769662 (100 μM), AICAR (1 mM) or metformin (1 mM). A-769662 robustly increased phosphorylation of AMPK and its downstream target ACC (Fig. 1A-C) at both time points (Fig. 1E-G). AICAR caused a modest but statistically significant change in AMPK and ACC phosphorylation; however, metformin did not alter AMPK or ACC phosphorylation in the astrocytoma cells. Only A-769662 caused a change in eATP, which was increased approximately 3-fold compared to control at both time points (Fig. 1D-H). Importantly, intracellular ATP was not altered by A-769662 treatment (Fig. 1I), indicating that increased eATP is not a result of increased ATP supply. These data indicate that only A-769662 (at 100 μM) produces a large and persistent change in AMPK activity in astrocytoma cells causing release of ATP and increased eATP levels.

A-769662 produces a concentration-dependent increase in eATP in U373 cells and mouse primary hypothalamic (HTAS) and cortical astrocytes (CRTAS)

To determine whether A-769662 altered eATP levels in a concentration-dependent manner, U373 cells and mouse primary HTAS and CRTAS cells were exposed to increasing concentrations of A-769662. Treatment of U373 cells with A-769662 for 30 minutes produced a biphasic response, with a decrease in eATP occurring at 25 μM, whereas concentrations greater than 50 μM increased eATP levels (Fig. 2A). A-769662 increased phosphorylation of AMPK and ACC in a

concentration-dependent manner (Fig. 2B). HTAS and CRTAS produced significantly less eATP at baseline, approximately 5-fold lower than U373 cells. However, in both cell types, A-769662 (>50 μM) increased eATP levels (Fig. 2C,E), although the AMPK and ACC phosphorylation response to A-769662 in HTAS (Fig. 2D) and CRTAS (Fig. 2F) was modest compared to U373 cells. These data suggest that A-769662 produces comparable increases in eATP despite differing increases in AMPK and ACC phosphorylation.

A-769662-induced increases in eATP are partially compound C-sensitive but persist in AMPK α1/α2 null MEFs.

To determine whether the increase in eATP from astrocytes is mediated by AMPK, we pre-incubated cells in Compound C, a non-specific AMPK inhibitor (10 μM) for 15 minutes before treatment with A-769662. We chose lower concentrations of A-769662 (10μM and 50μM) for these studies to limit the pharmacological competition between A-769662 and Compound C. In U373 cells and HTAS, pre-incubation with Compound C significantly attenuated the A-769662-induced increase in eATP (Fig. 3A,B). There was a trend for reduced eATP in Compound C-treated cortical astrocyte (CRTAS) cells following A-769662 treatment, which did not reach statistical significance (Fig. 3C).

Given that Compound C inhibits several other molecules at or below the concentrations used in the present study (www.kinase-screen.mrc.ac.uk/kinase-inhibitors), we decided to also utilise MEFs deficient for both catalytic subunits of AMPK (α1/α2 null) to confirm the specificity and action of A-769662. In WT MEFs, A-769662 (50-100 μM) induced a concentration-dependent increase in eATP (up

to ~4-fold following 100 μM). AMPKα1/α2 null MEFs exhibited significantly lower eATP levels at baseline (>80% lower); however, A-769662 (50-100 μM) still induced an increase in eATP in these cells (Fig. 3D). When normalized to their respective baseline values, the fold change in eATP from AMPKα1/α2 null MEF cells was similar, or even enhanced at higher A-769662 concentrations (Fig. 3E). Similar to the U373 cells, treatment of WT or AMPKα1/α2 null MEF cells with AICAR or metformin for 30 minutes did not alter eATP levels (ESM Fig. 2A,B). Western blots confirmed that the AMPKα1/α2 null MEF cells were deficient of catalytic subunits (ESM Fig. 2C). To determine why AMPK null MEFs had significantly lower eATP, we examined the intracellular ATP in both WT and AMPK null MEFs. AMPK null cells had significantly less total ATP (~40% reduction, Fig. 3F), suggesting that, indirectly, AMPK contributes to maintenance of eATP levels by sustaining the intracellular ATP concentration. Finally, to confirm whether enhancing AMPK activity altered eATP, we reduced the A-769662 concentration (50 μM) to produce a comparable activation of AMPK to AICAR (2 mM) and co-applied both drugs to U373 cells. Importantly, A-769662 increased eATP levels and AMPK phosphorylation and when A-769662 and AICAR were applied together, AMPK phosphorylation was further increased by AICAR but eATP levels were not altered (Fig. 3G-I), indicating that AMPK is unlikely to play a role in A-769662 induced release of ATP.

A-769662 increases intracellular calcium in U373 cells, HTAS and CRTAS

Application of the gap junction blocker carbenoxolone did not prevent A-769662-induced ATP release (ESM Fig. 3), we therefore tested whether ATP release could be occurring through vesicular ATP release, which is dependent on changes in

intracellular calcium ($[Ca^{2+}]_i$)[23, 24]. We performed non-ratiometric calcium imaging using Fluo4 Ca^{2+}-sensitive dye. A-769662 rapidly elevated $[Ca^{2+}]_i$ levels in a sustained manner (~2 minutes) in U373 (Fig. 4A), HTAS cells (Fig. 4B), and to a lesser extent, CRTAS cells (Fig. 4C). Intracellular $[Ca^{2+}]$ was also increased by A-769662 in the AMPKα1/α2 null MEFs although the response appeared more variable (not shown). We therefore performed single cell ratiometric calcium imaging using Fura-2. This also enabled us to examine the effect of A-769662 when cells were plated at low seeding density, thus limiting autocrine/paracrine signalling and allowing us to determine whether A-769662-induced ATP release could activate P2 receptors to increase intracellular calcium. We found that in approximately 20% of AMPKα1/α2 null MEFs, A-769662 (100 μM) induced an increase in $[Ca^{2+}]_i$, designated as an increase in the 340/380 ratio of greater than 20% of baseline fluorescence (Fig. 4D,E). Isolated cells also demonstrated an increase in $[Ca^{2+}]_i$, suggesting that paracrine ATP signalling is unlikely to mediate the increase in $[Ca^{2+}]_i$ and that A-769662 increases $[Ca^{2+}]_i$ and ATP release in a cell autonomous manner. Moreover, these data indicate that A-769662 does not require functional AMPK to increase $[Ca^{2+}]_i$ levels.

Chelation of intracellular calcium with BAPTA-AM attenuates A-769662-induced increases in eATP

To determine whether the change in intracellular calcium was directly responsible for the increased release of ATP from astrocytes, we chelated $[Ca^{2+}]_i$ using BAPTA-AM (50 μM; 30 min pre-incubation). There was a non-significant trend for reduced A-769662 response in U373 cells treated with BAPTA-AM (Fig. 4F). However, in HTAS and CRTAS, eATP levels induced by A-769662 were

significantly lower following BAPTA-AM pre-treatment (Fig. 4G,H). Next, we pre-exposed U373 cells, HTAS and CRTAS to a calcium-free extracellular solution to determine whether entry of extracellular calcium was required for ATP release. Under these conditions, the A-769662-induced increase in eATP was not altered (ESM Fig. 4A-C), although we did note a non-significant trend towards increased basal eATP levels in calcium-free saline in HTAS and CRTAS. Moreover, A-769662 challenge increased intracellular calcium in U373 cells bathed in calcium free saline, suggesting that A-769662 induces release of calcium from intracellular stores (ESM Fig. 4D,E). To determine whether purinergic receptor activation was required for A-769662-induced ATP release, we incubated cells in a cocktail of P2R antagonists, PPADS, 5-BDBD and A-438079. The presence of these inhibitors did not prevent A-769662 from increasing eATP levels (ESM Fig. 4F), suggesting that purinergic receptor activation is not required. Taken together these data suggest that release of calcium from intracellular stores contributes to the release of ATP induced by A-769662 by a mechanism that does not require purinergic receptor activation.

A-769662 increases eATP levels in several endocrine cell types

To examine whether the effect of high concentrations of A-769662 to alter ATP release is a general phenomenon across cell types, we performed concentration-response studies in a variety of other central and peripheral cell types including mouse glucose sensing neurons (GT1-7), human neuroblastoma cells (SH-SY5Y), murine BV-2 microglia, rat hepatoma cells (H4IIE), mouse myoblasts (C2C12) and rat pancreatic insulinoma cells (INS-1). We found that basal eATP levels varied across the cell types by nearly 10–fold (10-100 pmol/ml) but in every cell type

examined, A-769662 induced a significant increase in ATP release (Fig 5A-F). These data indicate that A-769662 also increases ATP release from other neural cell types namely neurons and microglia, as well as from peripheral cells including liver, muscle and pancreatic beta cell lines.

A-769662 reduces ECAR in an AMPK-dependent and AMPK-independent manner

AMPK is known to oppose the Warburg effect[25], essentially driving energy production through (more efficient) oxidative phosphorylation. Therefore, to determine whether A-769662 altered aspects of cellular metabolism by AMPK-dependent or AMPK-independent means, we utilised the Seahorse Extracellular flux analyser and exposed U373, WT MEF and AMPK $\alpha1/\alpha2$ null MEF cells to A-769662. Over time, higher concentrations (50–100 μM) of A-769662 caused ECAR to decrease in U373 (ESM Fig. 5A,C), WT MEFs (ESM Fig. 5D,F) and AMPK $\alpha1/\alpha2$ null MEFs (ESM Fig. 5G,I). Importantly, the highest concentration of A-769662 also reduced ECAR in AMPK null MEFs, although the magnitude of the response was reduced. OCR was not significantly altered in any cell type (ESM Fig. 5B,E,H). These data indicate that the reduction in ECAR induced by A-769662 has AMPK-dependent and AMPK-independent components.

Discussion

Astrocytes are the main source of extracellular ATP within the brain[26] and given that AMPK acts to maintain intracellular ATP levels, we hypothesised that AMPK may regulate ATP release from astrocytes. We postulated that activation of AMPK would limit ATP release, thus maintaining the pool of ATP available for metabolism. In contrast, we found that the commonly used AMPK activator drug A-769662 produced concentration-dependent increases in eATP levels in human astrocytoma (U373) cells, mouse primary astrocytes and several other central and peripheral endocrine cell types including liver, muscle and pancreatic beta cells. This occurred without substantial increases in intracellular ATP suggesting that eATP is not increasing as a consequence of increased intracellular ATP availability, but due to increased release.

A-769662 produced a large increase in AMPK and ACC phosphorylation in U373 cells, with HTAS and CRTAS displaying more modest increases. A-769662 preferentially activates AMPK heterotrimers containing the β1-subunit[27], therefore the attenuated AMPK and ACC phosphorylation induced by A-769662 in these cells types may reflect the relative expression (or lack thereof) of AMPKβ1. AICAR at high concentrations (1-2 mM) did not alter ATP release in U373 cells despite a modest activation of AMPK. Importantly, we could enhance AMPK activation with co-treatment of U373 cells with both A-769662 and AICAR, however, this did not enhance eATP levels, suggesting that ATP release is not a consequence of AMPK activity reaching a threshold. Metformin was without effect on eATP or AMPK phosphorylation in U373 cells, CRTAS and MEF WT or MEF AMPKα1/α2 null cells, most likely due to insufficient accumulation of metformin

into the intracellular compartment, possibly mediated by low organic cation transporter 1 expression[28]. AMPK inhibitor Compound C significantly reduced A-769662-induced ATP release in U373 cells at concentrations of A-769662 of <50 μM, however, higher concentrations of A-769662 still increased ATP release (not shown), suggesting that A-769662 can pharmacologically outcompete the effect of Compound C. To definitively test whether A-769662-induced ATP release was AMPK dependent, we utilised MEFs null for the AMPK catalytic subunits α1 and α2. In these cells, A-769662 produced a significant increase in eATP levels, which was not compound C-sensitive (not shown). Interestingly, basal eATP levels from AMPK null MEFs were >80% lower than WT cells, mediated by a ~40% decrease in intracellular ATP. These data suggest that AMPK may contribute to eATP levels simply by maintaining intracellular ATP levels.

Our data suggest that A-769662-induced increases in eATP are mediated by vesicular release, a process which is calcium-dependent[23, 24], as chelation of intracellular calcium using BAPTA-AM, diminished eATP levels in primary astrocyte cultures, with a non-significant trend toward reduced release in the U373 cells. Removal of extracellular calcium did not alter the A-769662-induced ATP release, indicating that entry of extracellular calcium is not required for this process. We went on to investigate whether A-769662-mediated ATP release could activate P2 receptors via paracrine signalling, which could alter both ATP release (i.e. ATP-induced ATP release) or change intracellular calcium. Using single cell ratiometric calcium imaging, we showed that A-769662 increased $[Ca^{2+}]_i$ when cells were bathed in calcium-free saline suggesting that P2X receptors are not contributing to increased $[Ca^{2+}]_i$ levels. When cells were present

at low density with constant perfusion, a situation where autocrine/paracrine signalling is negligible, we found that the A-769662-induced increase in $[Ca^{2+}]_i$ persisted, thus also ruling out a role for P2Y receptors. To determine more conclusively whether P2 receptor activation was important for A-769662-induced ATP release, we used a combination of a broad-spectrum P2 receptor blocker PPADS, which has a low affinity for P2X4 and P2X7[29], with P2X4 antagonist 5-BDBD and P2X7 antagonist A-438079. Under these conditions, the A-769662-induced ATP release from U373 cells remained. Taken together, these data suggest that A-769662 may increase calcium release from intracellular stores to induce ATP release, in a cell autonomous manner not requiring activation of P2Rs.

There are several potential consequences of increased ATP release induced by A-769662 that may complicate the interpretation of data utilising this drug as an AMPK activator in diabetes/metabolism studies. Release of ATP is a physiologically regulated process that occurs when cells experience a change in their environment. In the brain, ATP released from astrocytes is involved in stimulating breathing following changes in the partial pressure of CO_2 [30] and can contribute to left ventricular hypertrophy in a model of myocardial infarction in rats[31]. In muscle, eATP can enhance glucose uptake in a P2Y receptor-dependent mechanism, that induces GLUT4 translocation to the membrane.[32] Chronically elevated levels of ATP have been reported to induce insulin resistance in cultured adipocytes[33], and in blood extracellular ATP can enhance the release of mature IL-1β from macrophages, via a P2X7 receptor-dependent mechanism[34]. ATP can be broken down in the extracellular space to form adenosine and recent evidence suggests that astrocyte-derived adenosine (released as ATP) can reduce food

intake via activation of AgRP neuron adenosine A1 receptors[18]. Adenosine can also increase glucose uptake in mouse neurons and astrocytes via activation of the adenosine 2B receptor[35].

In conclusion, our data do not support a role for AMPK in acutely regulating ATP release from astrocytes. Instead, we find that complete loss of AMPK activity, mediated by knockout of both catalytic subunits, reduced eATP levels by reducing intracellular ATP levels. Moreover, A-769662 stimulated ATP release from cells by raising intracellular calcium levels derived from intracellular stores, an effect that persisted in the absence of AMPK activity and when purinergic receptor activation was minimised. Therefore, A-769662 promotes a signalling pathway(s) resulting in modified ATP release from peripheral and central cells, which is dependent on increased intracellular calcium. The release of ATP into the extracellular space caused by this drug may have an impact on alternative pathways including cellular glucose utilisation, inflammation and whole body energy metabolism, independently of AMPK activity.

Author contributions

J.M.V.W, J.L.R., A.M.C, A.M., P.G.W.P. and C.B. researched data. M.L.J.A., R.J.M., K.L.J.E. and C.B. contributed to experimental design. C.B. conceived the study and is the guarantor of the data.

Conflict of Interest

The authors have no conflict of interest to declare.

Acknowledgements

This study was funded by: Diabetes UK RD Lawrence Fellowship (13/0004647 to C.B.), British Society for Neuroendocrinology, Society for Endocrinology, Mary Kinross Charitable Trust and Tenovus Scotland. We thank Dr Benoit Viollet for kindly providing the AMPKα1/α2 null and WT MEFs, Dr Olumayokun Olajide for kindly providing the BV-2 cells and Dr Graham Rena and Dr Amy Cameron for kindly providing the C2C12 and H4IIE cells. We also wish to thank John Chilton, Holly Hardy and Andy Randall for technical assistance.

References

[1] Martinez de Morentin PB, Urisarri A, Couce ML, Lopez M. Molecular mechanisms of appetite and obesity: a role for brain AMPK. Clin Sci (Lond). 2016; **130**: 1697-1709

[2] Carling D, Zammit VA, Hardie DG. A common bicyclic protein kinase cascade inactivates the regulatory enzymes of fatty acid and cholesterol biosynthesis. FEBS Lett. 1987; **223**: 217-222

[3] Inoki K, Zhu T, Guan K-L. TSC2 Mediates Cellular Energy Response to Control Cell Growth and Survival. Cell. 2003; **115**: 577-590

[4] Merrill GF, Kurth EJ, Hardie DG, Winder WW. AICA riboside increases AMP-activated protein kinase, fatty acid oxidation, and glucose uptake in rat muscle. American Journal of Physiology-Endocrinology and Metabolism. 1997; **36**: E1107-E1112

[5] Minokoshi Y, Alquier T, Furukawa N*, et al.* AMP-kinase regulates food intake by responding to hormonal and nutrient signals in the hypothalamus. Nature. 2004; **428**: 569-574

[6] Andersson U, Filipsson K, Abbott CR*, et al.* AMP-activated protein kinase plays a role in the control of food intake. Journal of Biological Chemistry. 2004; **279**: 12005-12008

[7] McCrimmon RJ, Shaw M, Fan X*, et al.* Key role for AMP-activated protein kinase in the ventromedial hypothalamus in regulating counterregulatory hormone responses to acute hypoglycemia. Diabetes. 2008; **57**: 444-450

[8] Franke H, Verkhratsky A, Burnstock G, Illes P. Pathophysiology of astroglial purinergic signalling. Purinergic Signalling. 2012; **8**: 629-657

[9] Ferrari D, Wesselborg S, Bauer MKA, Schulze-Osthoff K. Extracellular ATP Activates Transcription Factor NF- κ B through the P2Z Purinoreceptor by Selectively Targeting NF- κ B p65 (RelA). The Journal of Cell Biology. 1997; **139**: 1635-1643

[10] Horvath TL, Sarman B, García-Cáceres C*, et al.* Synaptic input organization of the melanocortin system predicts diet-induced hypothalamic reactive gliosis and obesity. Proceedings of the National Academy of Sciences. 2010; **107**: 14875-14880

[11] Thaler JP, Yi C-X, Schur EA*, et al.* Obesity is associated with hypothalamic injury in rodents and humans. The Journal of Clinical Investigation. 2012; **122**: 153-162

[12] Buckman LB, Thompson MM, Moreno HN, Ellacott KL. Regional astrogliosis in the mouse hypothalamus in response to obesity. J Comp Neurol. 2013; **521**: 1322-1333

[13] Schur EA, Melhorn SJ, Oh S-K*, et al.* Radiologic evidence that hypothalamic gliosis is associated with obesity and insulin resistance in humans. Obesity. 2015; **23**: 2142-2148

[14] Buckman LB, Thompson MM, Lippert RN, Blackwell TS, Yull FE, Ellacott KLJ. Evidence for a novel functional role of astrocytes in the acute homeostatic response to high-fat diet intake in mice. Molecular Metabolism. 2015; **4**: 58-63

[15] Reiner DJ, Mietlicki-Baase EG, McGrath LE*, et al.* Astrocytes Regulate GLP-1 Receptor-Mediated Effects on Energy Balance. The Journal of Neuroscience. 2016; **36**: 3531-3540

[16] García-Cáceres C, Quarta C, Varela L*, et al.* Astrocytic Insulin Signaling Couples Brain Glucose Uptake with Nutrient Availability. Cell. **166**: 867-880
[17] Kim JG, Suyama S, Koch M*, et al.* Leptin signaling in astrocytes regulates hypothalamic neuronal circuits and feeding. Nat Neurosci. 2014; **17**: 908-910
[18] Yang L, Qi Y, Yang Y. Astrocytes control food intake by inhibiting AGRP neuron activity via adenosine A1 receptors. Cell reports. 2015; **11**: 798-807
[19] Buckman LB, Thompson MM, Lippert RN, Blackwell TS, Yull FE, Ellacott KL. Evidence for a novel functional role of astrocytes in the acute homeostatic response to high-fat diet intake in mice. Mol Metab. 2015; **4**: 58-63
[20] Zhang X, Zhang G, Zhang H, Karin M, Bai H, Cai D. Hypothalamic IKK β /NF-κ B and ER Stress Link Overnutrition to Energy Imbalance and Obesity. Cell. 2008; **135**: 61-73
[21] Fantino M, Wieteska L. Evidence for a direct central anorectic effect of tumor-necrosis-factor-alpha in the rat. Physiology & Behavior. 1993; **53**: 477-483
[22] Dhillon H, Zigman JM, Ye C*, et al.* Leptin directly activates SF1 neurons in the VMH, and this action by leptin is required for normal body-weight homeostasis. Neuron. 2006; **49**: 191-203
[23] Zhang J, Kornecki E, Jackman J, Ehrlich YH. ATP secretion and extracellular protein phosphorylation by CNS neurons in primary culture. Brain Research Bulletin. 1988; **21**: 459-464
[24] Bal-Price A, Moneer Z, Brown GC. Nitric oxide induces rapid, calcium-dependent release of vesicular glutamate and ATP from cultured rat astrocytes. Glia. 2002; **40**: 312-323
[25] Faubert B, Boily G, Izreig S*, et al.* AMPK Is a Negative Regulator of the Warburg Effect and Suppresses Tumor Growth In Vivo. Cell Metabolism. 2013; **17**: 113-124
[26] Coco S, Calegari F, Pravettoni E*, et al.* Storage and Release of ATP from Astrocytes in Culture. Journal of Biological Chemistry. 2003; **278**: 1354-1362
[27] Scott JW, van Denderen BJW, Jorgensen SB*, et al.* Thienopyridone Drugs Are Selective Activators of AMP-Activated Protein Kinase β 1-Containing Complexes. Chemistry & Biology. 2008; **15**: 1220-1230
[28] Wang DS, Jonker JW, Kato Y, Kusuhara H, Schinkel AH, Sugiyama Y. Involvement of organic cation transporter 1 in hepatic and intestinal distribution of metformin. The Journal of pharmacology and experimental therapeutics. 2002; **302**: 510-515
[29] Khakh BS, North RA. Neuromodulation by Extracellular ATP and P2X Receptors in the CNS. Neuron. 2012; **76**: 51-69
[30] Gourine AV, Kasymov V, Marina N*, et al.* Astrocytes Control Breathing Through pH-Dependent Release of ATP. Science. 2010; **329**: 571-575
[31] Marina N, Tang F, Figueiredo M*, et al.* Purinergic signalling in the rostral ventro-lateral medulla controls sympathetic drive and contributes to the progression of heart failure following myocardial infarction in rats. Basic Res Cardiol. 2012; **108**: 1-10
[32] Osorio-Fuentealba C, Contreras-Ferrat AE, Altamirano F*, et al.* Electrical Stimuli Release ATP to Increase GLUT4 Translocation and Glucose Uptake via PI3K γ -Akt-AS160 in Skeletal Muscle Cells. Diabetes. 2013; **62**: 1519-1526
[33] Yu Z, Jin T. Extracellular high dosages of adenosine triphosphate induce inflammatory response and insulin resistance in rat adipocytes. Biochemical and Biophysical Research Communications. 2010; **402**: 455-460

[34] Perregaux DG, McNiff P, Laliberte R, Conklyn M, Gabel CA. ATP Acts as an Agonist to Promote Stimulus-Induced Secretion of IL-1 β and IL-18 in Human Blood. The Journal of Immunology. 2000; **165**: 4615-4623
[35] Lemos C, Pinheiro BS, Beleza RO*, et al.* Adenosine A2B receptor activation stimulates glucose uptake in the mouse forebrain. Purinergic Signalling. 2015; **11**: 561-569

Figure Legends

Figure 1. A-769662 potently activates AMPK and stimulates ATP release from U373 cells. **A**. Representative immunoblots from U373 cells treated with A-769772 (100 μM), AICAR (1 mM) or metformin (1 mM) for 30 minutes (n=8-9). Densitometric analysis for pT172 AMPK and pS79 ACC depicted in **B** and **C**, respectively. **D**. Analysis of extracellular ATP (eATP; n=8). **E**. Representative immunoblots from U373 cells treated with A-769662, AICAR and metformin for 3 hours, with densitometric analysis shown for pT172 AMPK and pS79 ACC shown in **F** and **G**, respectively (n=8). Analysis of eATP for 3 hour treatments shown in **H** (n=8). **I**. Analysis of intracellular ATP (iATP) levels in U373 cells following 30 minutes of A-769662 treatment (n=7). *p<0.05

Figure 2. A-769662 concentration-dependently increases eATP from U373 cell and primary mouse hypothalamic and cortical astrocytes. A. Treatment of U373 cells with increasing concentrations of A-769662 for 30 minutes increases eATP (n=6), with representative immunoblots of pT172 AMPK, pS79 ACC and actin depicted in **B. C.** Treatment of primary hypothalamic astrocytes (HTAS; n=5) with increasing concentrations of A-769662 for 30 minutes also increases eATP levels, with representative immunoblots depicted in **D. E.** Treatment of primary cortical astrocytes (CRTAS; n=9) with increasing concentrations of A-769662 for 30 minutes also increased eATP levels, with representative immunoblots depicted n **F**. *p<0.05;**p<0.01; ***p<0.001

Figure 3. Compound C pre-treatment attenuates A-769662-induced increases in eATP but still persists in AMPK α1/α2 null mouse embryonic

fibroblasts (MEF). Pre-treatment of cells with Compound C (10 μM; 15 mins) prevented A-769662-induced increases in eATP in U373 (**A**; n=6) and HTAS (**B**; n=4), with a non-significant trend toward reduced release in CRTAS (**C**; n=5). **D**. Treatment of MEFs with A-769662 caused a concentration-dependent increase in eATP from WT and AMPK null MEFs. **E**. eATP levels from D normalised to baseline for each cell type. **F**. Intracellular ATP levels in WT versus AMPK null MEFs. **G**. Measurement of eATP following treatment of U373 cells with A-769662 (50 μM) in the absence and presence of AICAR (2 mM; n=6). **H**. Representative immunoblots from G. **I**. Densitometric analysis from H. **p*<0.05;***p*<0.01;****p*<0.001; *$* vs vehicle; *#* vs WT.

Figure 4. A-769662 increases intracellular calcium and chelation of intracellular calcium diminishes the A-769662-induced increase in eATP. A-C. Cells were loaded with Fluo4 direct for 60 minutes. Injection of A-769662 (100 μM; at 0.5 min) increased the relative fluorescence (RFU) in U373 (**A**; n=3), HTAS (**B**; n=4) and CRTAS (**C**; n=4). Cells were also injected with 0.1% (v/v) DMSO as control (Cont). **D**. A representative trace of ratiometric calcium imaging using Fura-2 in AMPK α1/α2 null MEF cells. 340/380 ratios were normalised to 1 to correspond with Fluo4 data. Mean relative fluorescence units from a field of 9 AMPK α1/α2 null MEF cells. **E**. Representative images of ratiometric calcium signals before and after A-769662 treatment in AMPK α1/α2 null MEF cells. **F**. Pre-incubation of cells with BAPTA-AM (50 μM) for 30 minutes prior to A-769662 addition did not significantly alter eATP levels from U373 cells (n=8). BAPTA-AM

pre-treatment significantly reduced A-769662-induced eATP levels in HTAS (**G**; n=5) and CRTAS (**H**; n=6). *p<0.05; **p<0.01;***p<0.001

Figure 5. A-769662 increases eATP in a number of other endocrine cells. A-769662 increased eATP levels from mouse glucosensing hypothalamic GT1-7 neurons (**A**; n=5), human Sh-SY5Y neuroblastoma cells (**B**; n=6), murine BV-2 microglia (**C**; n=7), rat hepatoma H4IIE cells (**D**; n=6), mouse C2C12 myoblasts (**E**; n=9) and rat pancreatic beta cell INS-1E cells (**F**; n=4). *p<0.05; **p<0.01;***p<0.001

ESM Figure 1. Validation of mouse primary astrocyte cultures. Top row: Primary cortical astrocyte (CRTAS) stained with DAPI (nuclear stain), glial fibrillary acidic protein (GFAP) and Iba1 (microglial marker). CRTAS cultures had >80% GFAP positive cells and <2% Iba1-positive cells. Bottom row: Primary hypothalamic astrocyte (HTAS) cultures stained with DAPI, GFAP and Iba1. HTAS cultures had >85% GFAP-positive cells and <2% Iba1-positive cells.

ESM Figure 2. Metformin and AICAR do not alter eATP levels in MEF WT or MEF AMPK α1/α2 null cells. A. Analysis of extracellular ATP (eATP) from wild type mouse embryonic fibroblasts (MEF WT) treated with A-769662 (100 μM), AICAR (1 mM) or metformin (1 mM) for 30 minutes (n=5). **B**. Analysis of eATP from MEF AMPKα1/α2 null cells following treatment with A-769662, AICAR and metformin, as above (n=5). **C**. Representative immunoblot of MEF WT and AMPK α1/α2 null cells treated with A-769662 (100 μM), AICAR (1 mM) and metformin

(1 mM) for 30 minutes and probed for pT172 AMPK and actin (n=3). **p<0.01; ***p<0.001

ESM Figure 3. Gap junction blockade with carbenoxolone did not prevent A-769662-induced increases in eATP. A. Pre-treatment of U373 cells with carbenoxolone (100 μM) significantly enhanced A-769662 (100 μM)-induced eATP levels (n=3). Pre-treatment of HTAS (**B**; n=4) and CRTAS (**C**; n=5) with carbenoxlone did not significantly alter A-769662-induced increases in eATP levels. *p<0.05;**p<0.01

ESM Figure 4. Incubation in calcium free saline did not prevent A-769662-induced increases in eATP or intracellular calcium and pharmacological blockage of purinergic receptors does not prevent A-769662-induced ATP release. Incubation of U373 cells (**A**; n=5), primary hypothalamic astrocytes (HTAS; **B**; n=8) or primary mouse cortical astrocytes (CRTAS; **C**; n=6) in an extracellular saline solution containing zero calcium did not attenuate the A-769662 (100 μM) induced increase in eATP. **D**. Representative ratiometric calcium imaging trace (one of 3 independent experiments) of U373 cells treated with A-769662 (100 μM) in calcium free saline (mean normalised relative fluorescence units of 29 cells). **E**. Representative images pre and post addition of A-769662. **F**. Analysis of eATP levels from U373 cells treated with A-769662 plus a cocktail of purinergic receptor antagonists (PPADS [100 μm]; 5-BDBD [5 μM]; A-438069 [100 μM]. *p<0.05;**p<0.01

Figure ESM 5. A-769662 decreases the extracellular acidification rate with AMPK-dependent and AMPK-independent components. A. Extracellular acidification rate (ECAR) normalised to baseline of U373 cells exposed to A-769662. **B**. Oxygen consumption rate (OCR) of U373 cells exposed to A-769662, normalised to baseline. **C**. Extrapolation of ECAR data approximately 90 mins post injection. **D**. ECAR normalised to baseline of WT MEF cells exposed to A-769662. **E**. Oxygen consumption rate (OCR) of WT MEF cells exposed to A-769662, normalised to baseline. **F**. Extrapolation of ECAR data approximately 90 mins post injection (n=14-16). **G**. ECAR normalised to baseline of AMPK α1/α2 null MEF cells exposed to A-769662. **H**. Oxygen consumption rate (OCR) of AMPK α1/α2 null MEF cells exposed to A-769662, normalised to baseline. **I.** Extrapolation of ECAR data approximately 90 minutes post injection. *p<0.05;**p<0.01;***p<0.001; n=14-16.

Figure 1

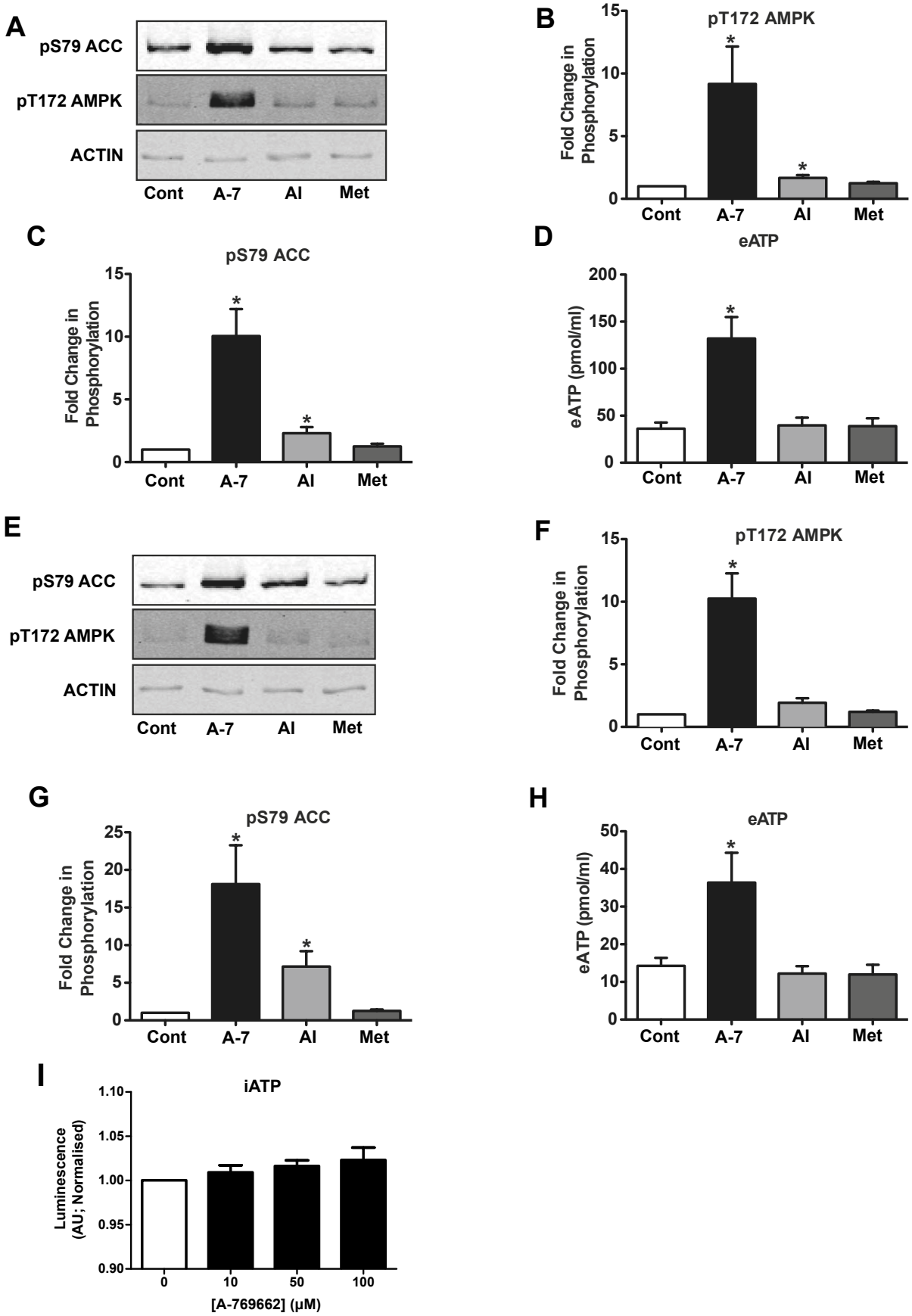

Figure 1. **A-769662 potently activates AMPK and stimulates ATP release from U373 cells. A**. Representative immunoblots from U373 cells treated with A-769662 (100 μM), AICAR (1 mM) or metformin (1 mM) for 30 minutes (n=8-9). Densitometric analysis for pT172 AMPK and pS79 ACC depicted in **B** and **C**, respectively. **D**. Analysis of extracellular ATP (eATP; n=8). **E**. Representative immunoblots from U373 cells treated with A-769662, AICAR and metformin for 3 hours, with densitometric analysis shown for pT172 AMPK and pS79 ACC shown in **F** and **G**, respectively (n=8). Analysis of eATP for 3 hours treatments shown in **H** (n=8). **I**. Analysis of intracellular ATP(iATP) levels in U373 cells following 30 minutes of A-769662 treatment (n=7). **p*<0.05

Figure 2

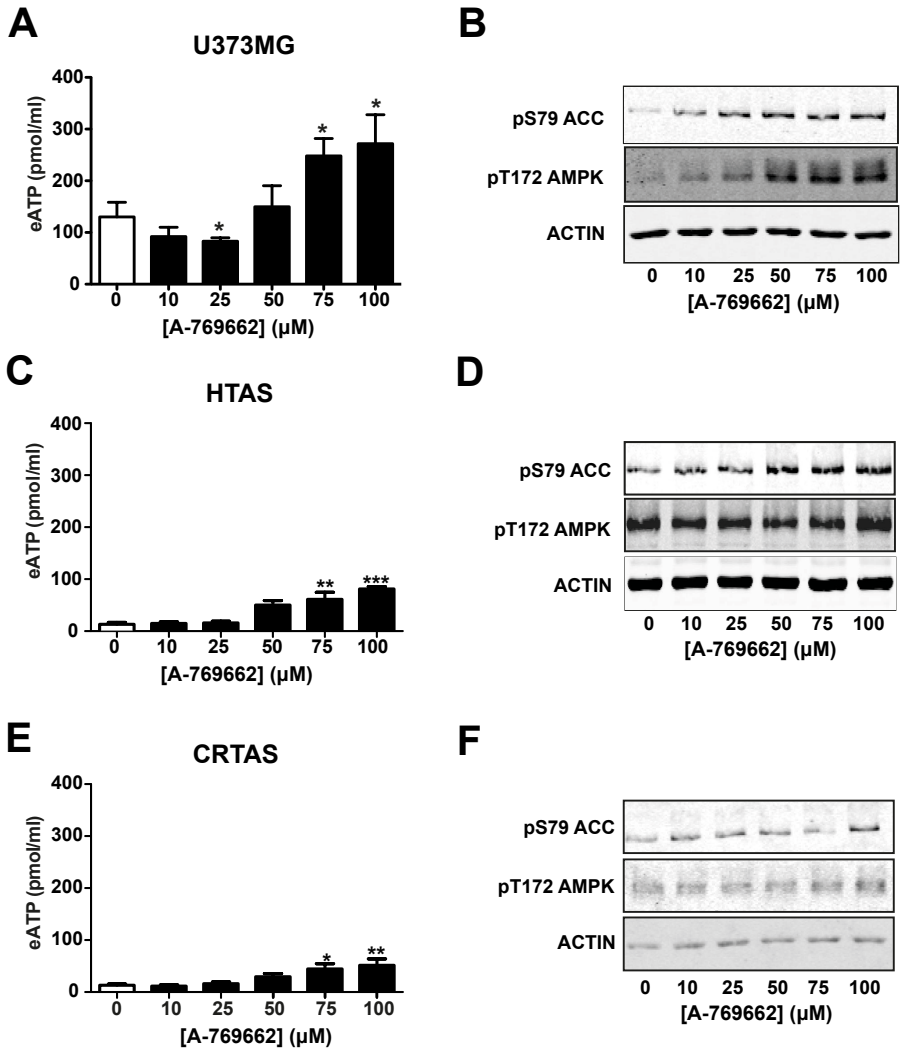

Figure 2. A-769662 concentration-dependently increases eATP from U373 cells and primary mouse hypothalamic and cortical astrocytes. A. Treatment of U373 cells with increasing concentrations of A-769662 for 30 minutes increases eATP (n=6), with representative immunoblots of pT172 AMPK, pS79 ACC and actin depicted in **B**. **C.** Treatment of primary hypothalamic astrocytes (HTAS; n=5) with increasing concentrations of A-769662 for 30 minutes also increases eATP levels, with representative immunoblots depicted in **D**. **E**. Treatment of primary cortical astrocytes (CRTAS; n=9) with increasing concentrations of A-769662 for 30 minutes also increased eATP levels, with representative immunoblots depicted in **F**. $p^*<0.05$; $^{**}p<0.01$; $^{***}p<0.001$

Figure 3

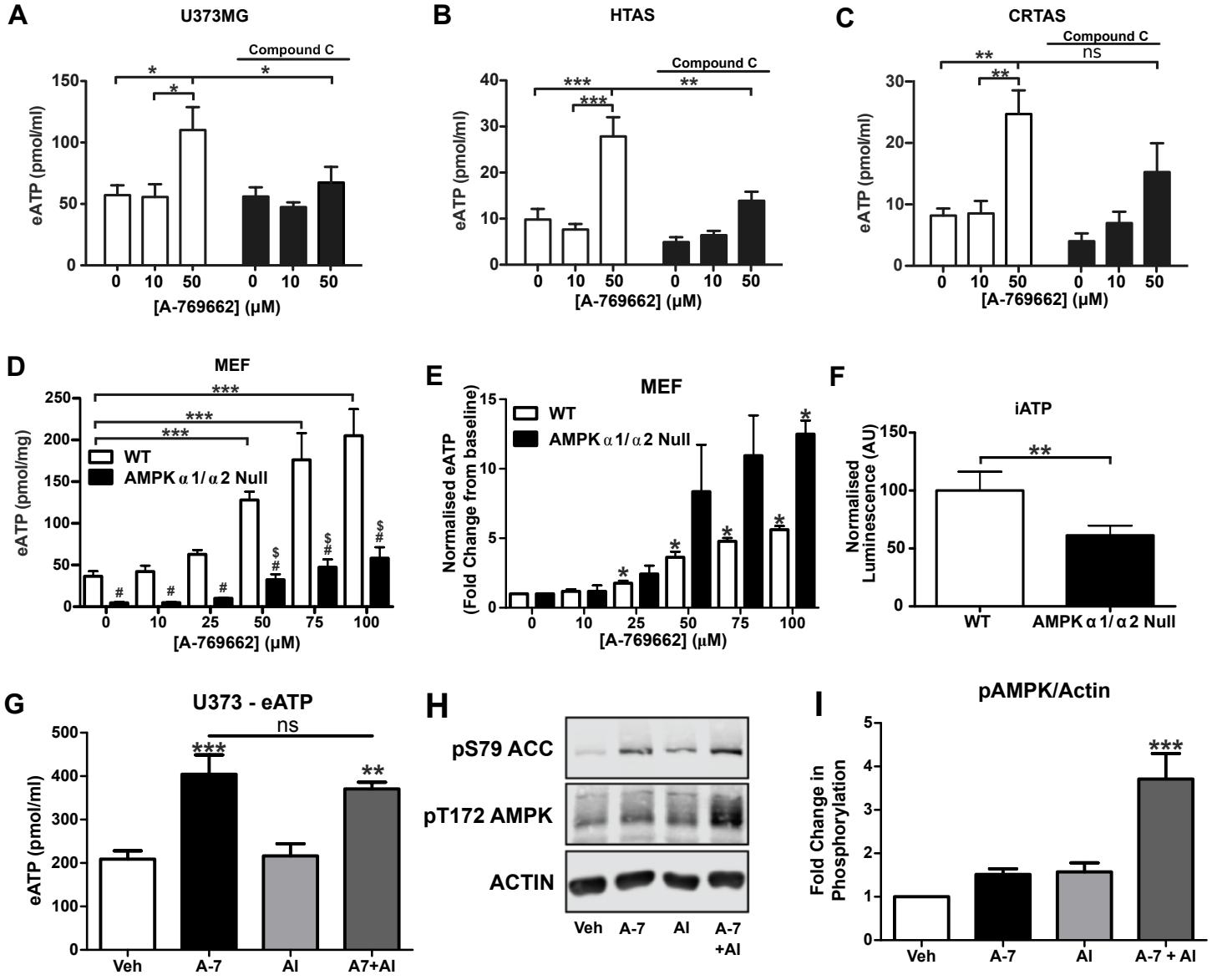

Figure 3. **Compound C pre-treatment attenuates A-769662-induced increases in eATP but still persists in AMPK α1/α2 null mouse embryonic fibroblasts (MEF).** Pre-treatment of cells with Compound C (10 μM; 15 mins) prevented A-769662-induced increases in eATP in U373 (**A**; n=6) and HTAS (**B**; n=4), with a non-significant trend toward reduced release in CRTAS (**C**; n=5). **D**. Treatment of MEFs with A-769662 caused a concentration-dependent increase in eATP from WT and AMPK null MEFs. **E**. eATP levels from D normalised to baseline for each cell type. **F**. Intracellular ATP levels in WT versus AMPK null MEFs. **G**. Measurement of eATP following treatment of U373 cells with A-769662 (100 μM) in the absence and presence of AICAR (2 mM; n=6). **H**. Representative immunoblots from G. **I**. Densitometric analysis from H. **p*<0.05;***p*<0.01;****p*<0.001; $ vs vehicle; # vs WT.

Figure 4

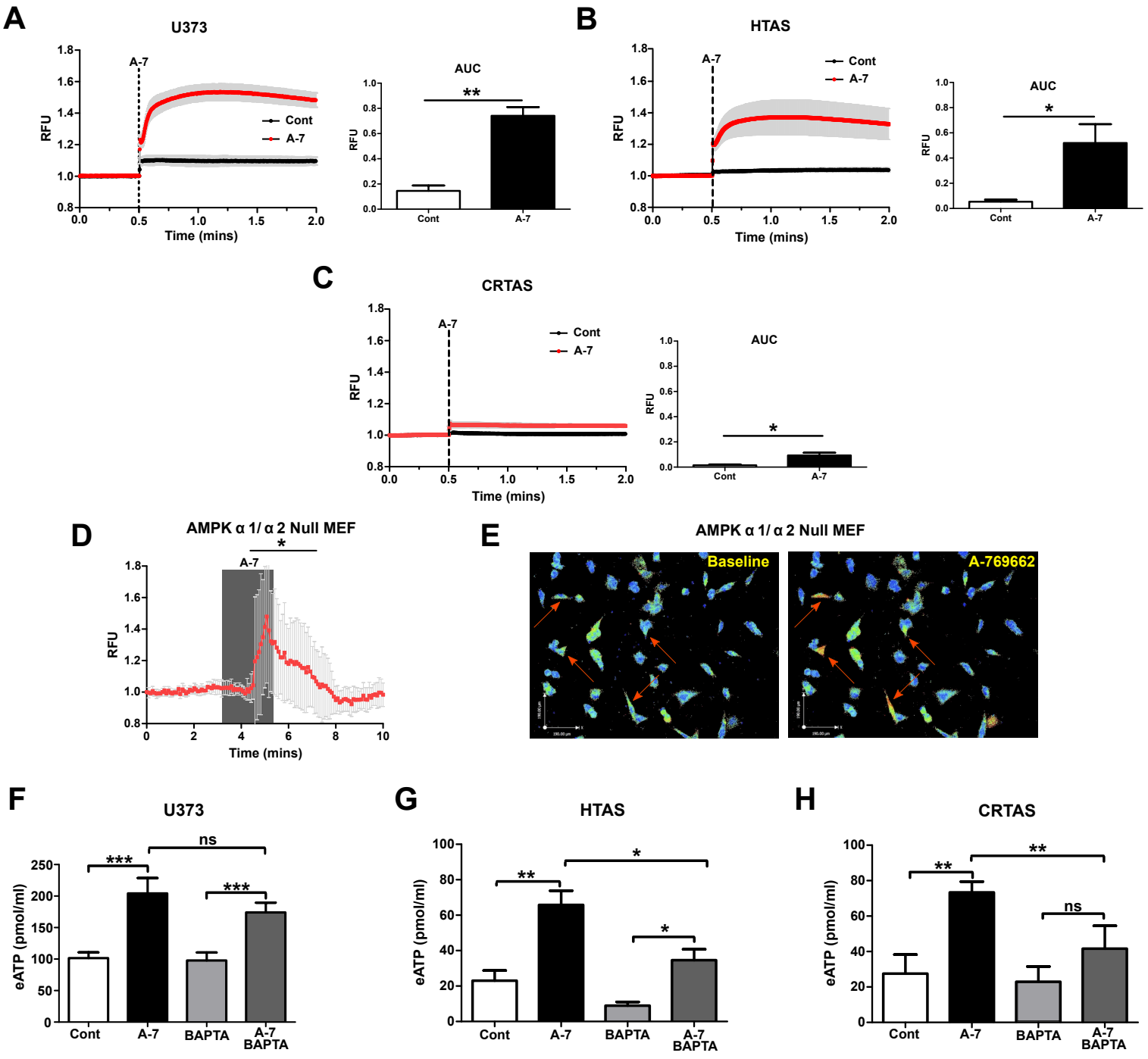

Figure 4. **A-769662 increases intracellular calcium and chelation of intracellular calcium diminishes the A-769662-induced increase in eATP**. **A-C.** Cells were loaded with Fluo4 direct for 60 minutes. Injection of A-769662 (100 μM; at 0.5 min) increased relative fluorescence (RFU) in U373 (**A**; n=3), HTAS (**B**; n=4) and CRTAS (**C**; n=4). Cells were also injected with 0.1% (v/v) DMSO as control (Cont). **D**. A representative trace of ratiometric calcium imaging using Fura-2 in AMPK α1/α2 null MEF cells. 340/380 ratios were normalised to 1 to correspond with Fluo4 data. Mean relative fluorescence units from a field of 9 AMPK KO MEF cells. **E**. Representative images of ratiometric calcium signals before and after A-769662 treatment in AMPK α1/α2 null MEF cells. **F**. Preincubation of cells with BAPTA-AM (50 μM) for 30 minutes prior to A-769662 addition did not significantly alter eATP levels from U373 cells (n=8). BAPTA-AM pre-treatment significantly reduced A-769662-induced eATP levels in HTAS (**G**; n=5) and CRTAS (**H**; n=6). **p*<0.05;***p*<0.01; ****p*<0.001

Figure 5

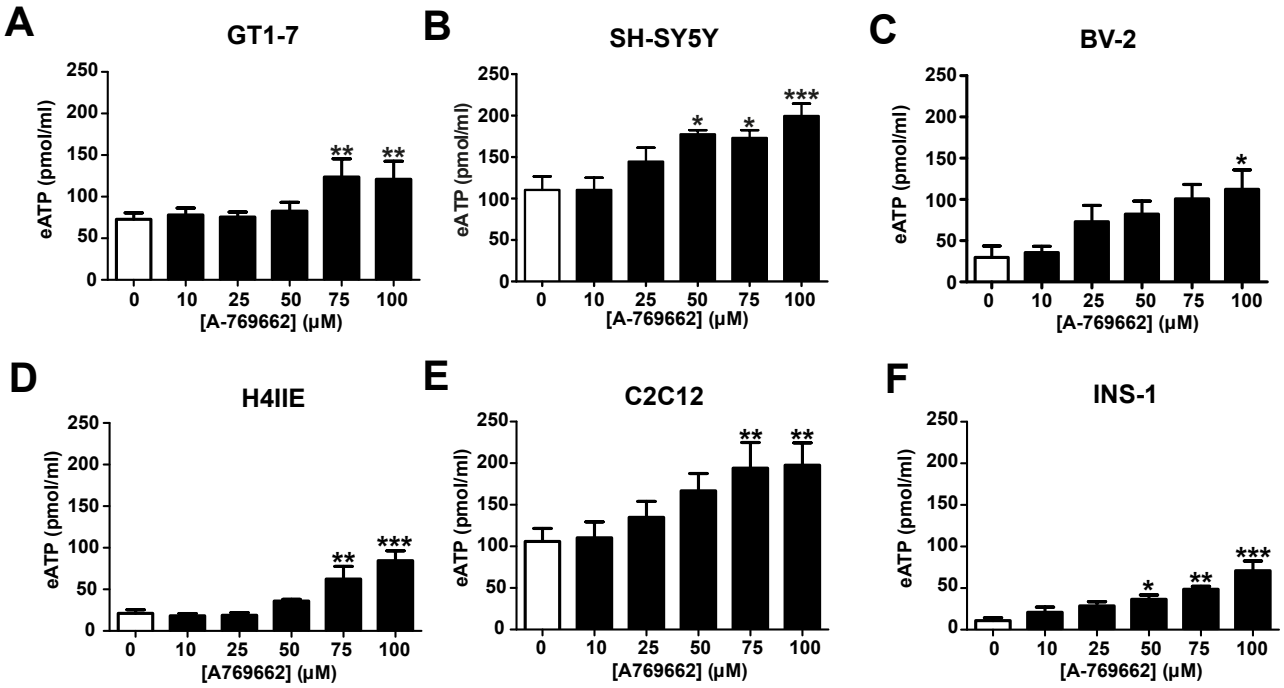

Figure 5. **A-769662 increases eATP in a number of other endocrine cells.** A-769662 increased eATP levels from mouse glucosensing hypothalamic GT1-7 neurons (**A;** n=5), human SH-SY5Y neuroblastoma cells (**B;** n=6), murine BV-2 microglia (**C;** n=7), rat hepatoma H4IIE cells (**D;** n=6), mouse C2C12 muscle myoblasts (**E;** n=9) and rat pancreatic beta cell INS-1 cells (**F;** n=4) **p*<0.05;***p*<0.01;****p*<0.001

ESM Figure 1

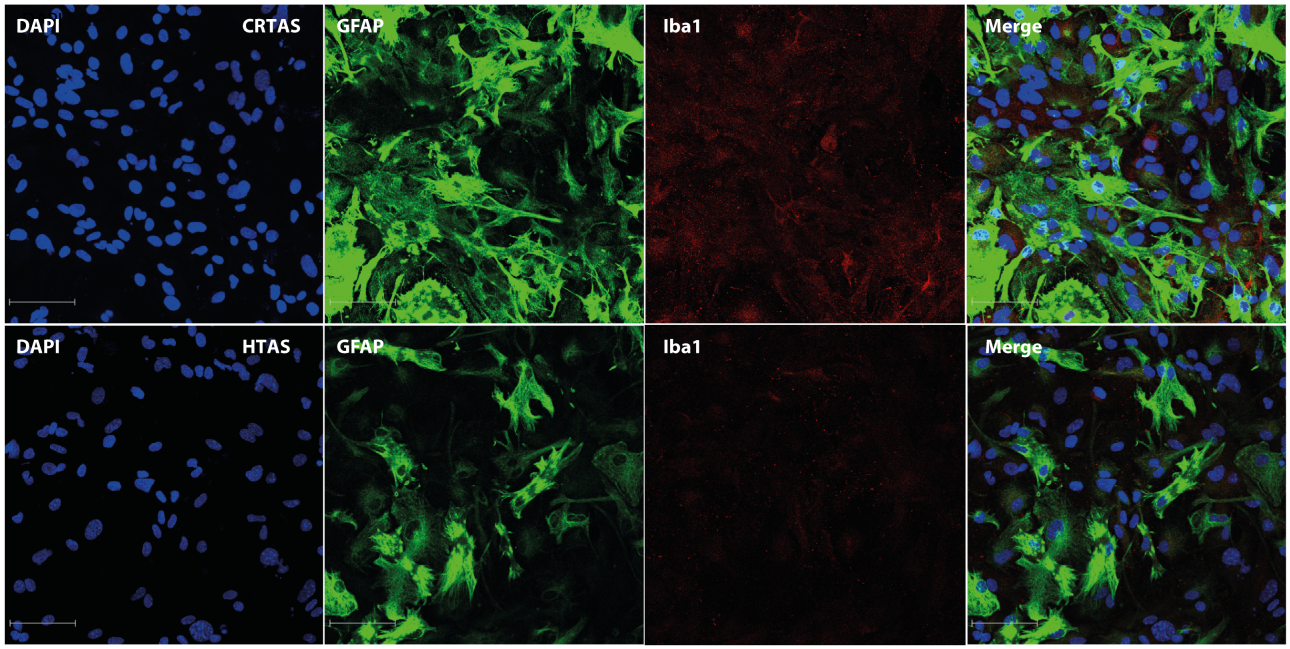

ESM Figure 1. **Validation of mouse primary astrocyte cultures.** Top row: Primary cortical astrocyte (CRTAS) cultures stained with DAPI (nuclear stain), glial fibrillary acidic protein (GFAP) and Iba1 (microglial marker). CRTAS cultures had >80% GFAP-positive cells and <2% Iba1-positive cells. Bottom row: Primary hypothalamic astrocyte (HTAS) cultures stained with DAPI, GFAP and Iba1. HTAS cultures had >85% GFAP-positive cells and less than 2% Iba1-positive cells.

ESM Figure 2

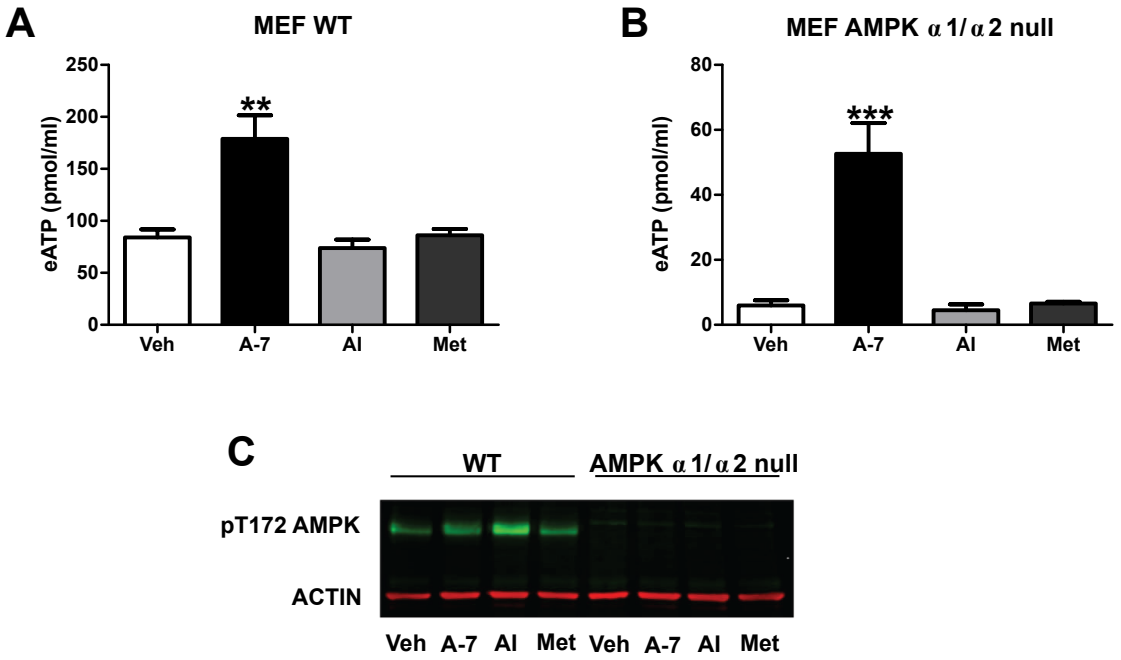

ESM Figure 2. **Metformin and AICAR do not alter eATP levels in MEF WT or MEF AMPK α1/α2 null cells. A**. Analysis of extracellular ATP (eATP) from wild type mouse embryonic fibroblasts (WT MEF) treated with A-769662 (100 μM), AICAR (1 mM) or metformin (1 mM) for 30 minutes (n=5). **B**. Analysis of eATP from MEF AMPK α1/α2 null cells following treatment with A-769662, AICAR and metformin, as above (n=5). **C**. Representative immunoblot of MEF WT and AMPK α1/α2 null cells treated with A-769662 (100 μM), AICAR (1 mM) and metformin (1 mM) for 30 minutes and probed for pT172 AMPK and actin (n=3). $^{**}p<0.01$;$^{***}p<0.001$

ESM Figure 3

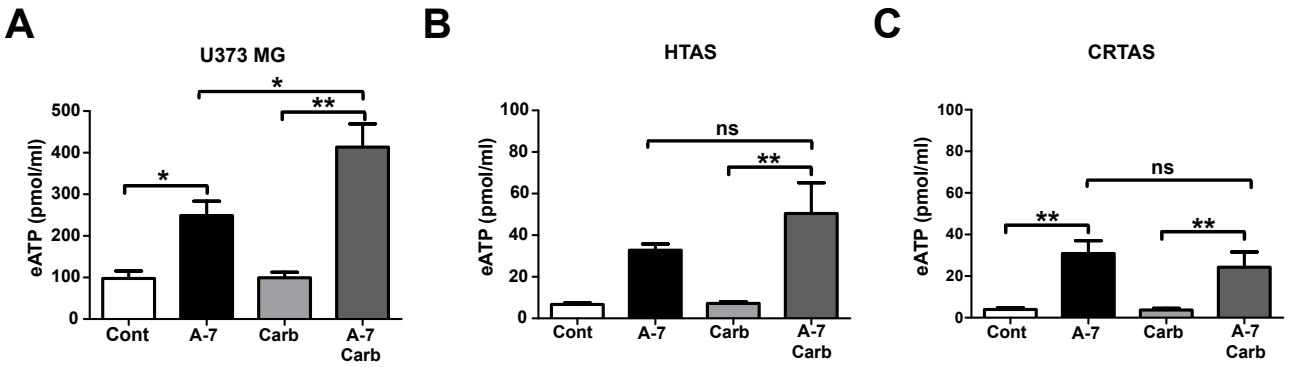

ESM Figure 3. **Gap junction blockade with carbenoxolone did not prevent A-769662-induced increases in eATP. A**. Pre-treatment of U373 cells with carbenoxolone (100 mM) significantly enhanced A-769662 (100 mM)-induced eATP levels (n=3). Pre-treatment of HTAS (**B**; n=4) and CRTAS (**C**; n=5) with carbenoxolone did not significantly alter A-769662-induced increases in eATP levels. *p<0.05;**p<0.01

ESM Figure 5

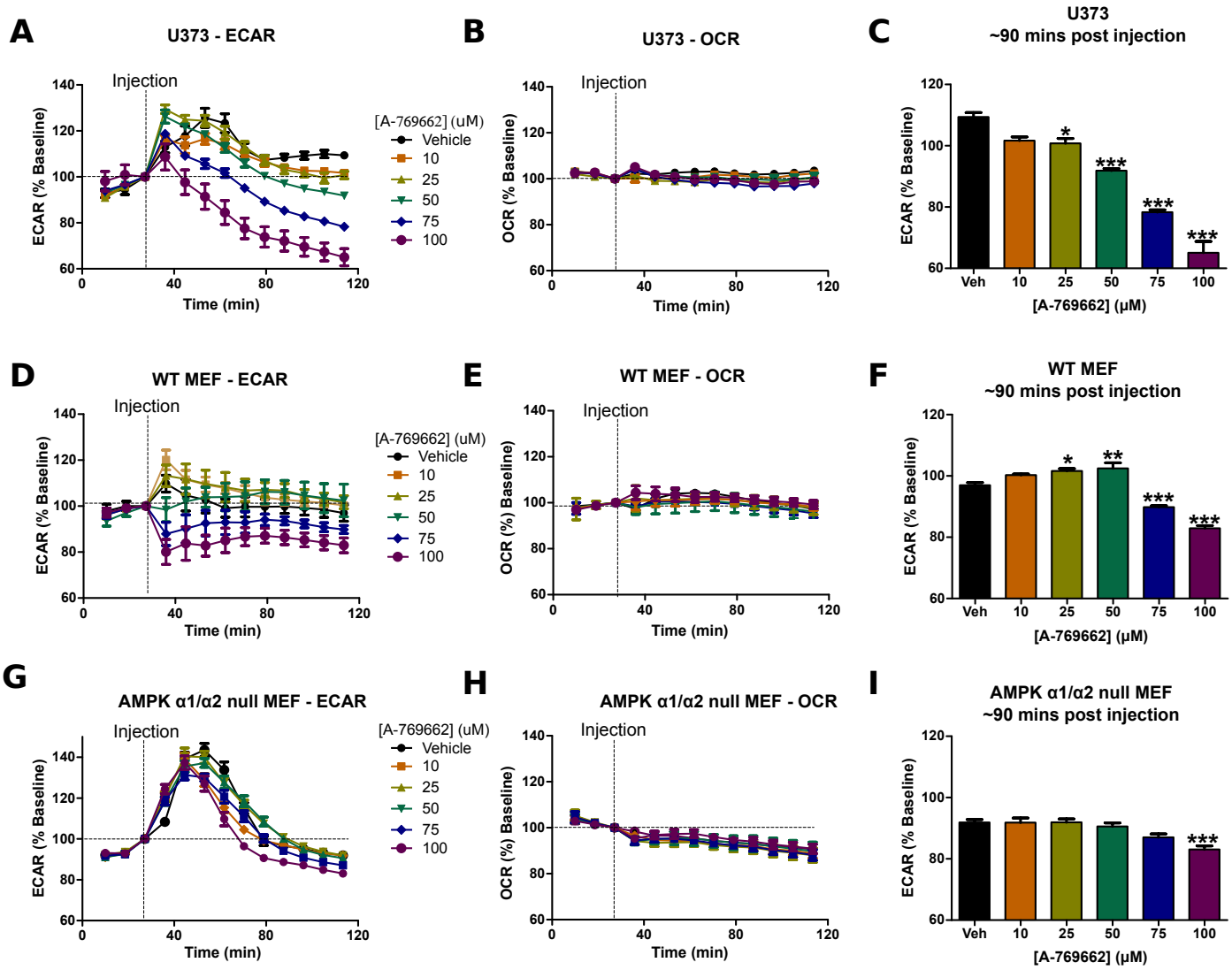

ESM Figure 5. A-769662 decreases the extracellular acidification rate with AMPK-dependent and AMPK-independent components. A. Extracellular acidification (ECAR), normalised to baseline of U373 cells exposed to A-769662**. B.** Oxygen consumption rate (OCR) of U373 cells exposed to A-769662, normalised to baseline. **C**. Extrapolation of ECAR data approximately 90 mins post injection. **D**. ECAR normalised to baseline of WT MEF cells exposed to A-769662. **E**. Oxygen consumption rate (OCR) of WT MEF cells exposed to A-769662, normalised to baseline. **F**. Extrapolation of ECAR data approximately 90 mins post injection. **G**. ECAR normalised to baseline of AMPK α1/α2 null MEF cells exposed to A-769662. **H**. Oxygen consumption rate (OCR) of AMPK α1/α2 null MEF cells exposed to A-769662, normalised to baseline. **I**. Extrapolation of ECAR data approximately 90 mins post injection. (*P<0.05;**P<0.01;***P<0.001; n=14-16)**.**

ESM Figure 4

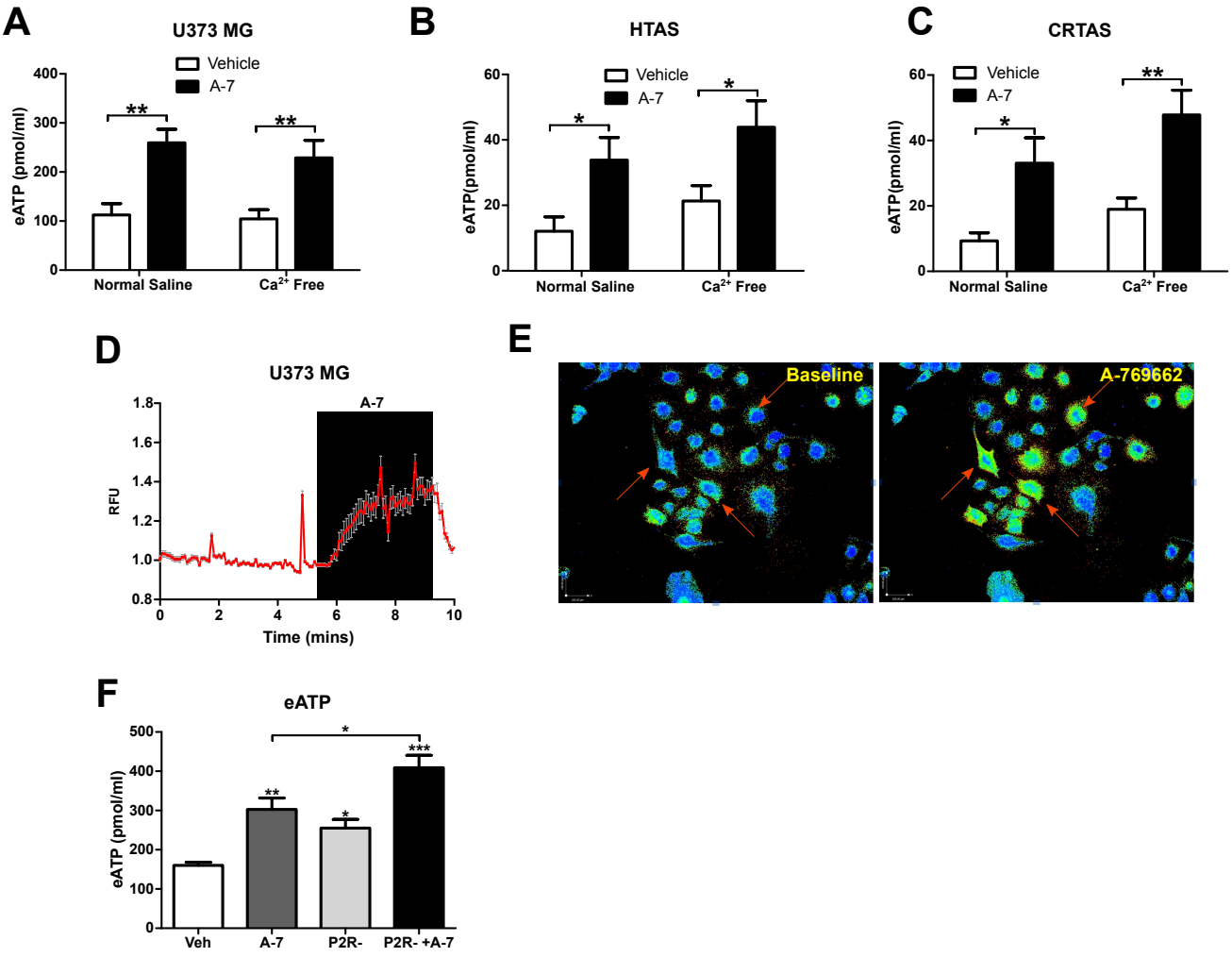

ESM Figure 4. **Incubation in calcium free saline did not prevent A-769662-induced increases in eATP or intracellular calcium and pharmacological blockade of purinergic receptors does not prevent A-769662-induced ATP release.** Incubation of U373 cells (**A**; n=5), primary hypothalamic astrocytes (HTAS; **B**; n=8) or primary mouse cortical astrocytes (CRTAS; **C**; n=6) in an extracellular saline solution containing zero calcium did not attenuate the A-769662 (100 μM) induced increase in eATP. **D**. Representative ratiometric calcium imaging trace (one of 3 independent experiments) of U373 cells treated with A-769662 (100 μM) in calcium free saline (mean normalised relative fluorescence units of 29 cells). **E**. Representative images pre and post addition of A-769662. **F**. Analysis of eATP levels from U373 cells treated with A-769662 plus a cocktail of purinergic receptor antagonists (PPADS [100 μM]; 5-BDBD [5 μM]; A-437069 [100 μM]. **p*<0.05;***p*<0.01;****p*<0.001